Eur. J. Mineral.
1994, **6**, 753-771

vX properties of CH_4-CO_2 and CO_2-N_2 fluid inclusions : modelling for $T < 31°C$ and $P < 400$ bars

RÉGIS THIÉRY*, ALFONSUS MARTINUS VAN DEN KERKHOF** and JEAN DUBESSY*

* CREGU, Centre de Recherche sur la Géologie des Matières Minérales et Energétiques, BP 23, 54501-Vandoeuvre-lès-Nancy Cedex, France

** Institute of Geology and Dynamics of the Lithosphere, University of Göttingen, Goldschmidtstraße 3, D-37077 Göttingen, Germany

Abstract: *vX* properties of the binary systems CO_2-CH_4 and CO_2-N_2 are described with improved accuracy and for the full ranges of composition and molar volume. *PTX* conditions of phase transitions including liquid, gas and solid are modelled by the Soave-Redlich-Kwong equation of state, and molar volumes by the Lee-Kesler correlation. The Soave-Redlich-Kwong equation of state has been improved for critical fluids. *vX* diagrams are presented, which describe phase transitions involving liquid, gas and CO_2 solid phases for CO_2-CH_4 and CO_2-N_2 fluid inclusions. Also discussed are the conditions of the metastable liquid-liquid-gas phase assemblage.

Key-words: fluid inclusions, CO_2-CH_4-N_2 system, phase equilibria, *vX* properties, equations of state.

Introduction

The determination of fluid compositions (*X*) and molar volumes (*v*) is an essential step for any quantitative study of paleo-fluids, presently found as relicts in fluid inclusions. Temperature measurements of phase transitions observed by microthermometry and combined with Raman spectrometry allow fairly accurate determinations of the *vX* properties of the non-aqueous volatile parts of fluid inclusions. As popularized by Burruss (1981), *vX* diagrams are most appropriate for quantitative interpretations of phase transitions in fluid inclusions. In many cases, non-aqueous volatile portions of fluid inclusions can be described in the CO_2-CH_4-N_2 system. Unfortunately, experimental data are not numerous enough for an accurate interpretation of phase equilibria, and molar volumes of CO_2-CH_4-N_2 fluids are poorly known. Thus, the accuracy of *vX* determinations mainly relies on the applied equations of state (EOS) and the derived phase diagrams. The large amounts of microthermometric and Raman data, produced during the last decade, have demonstrated that available phase diagrams for the CO_2-CH_4 system (Herskowitz & Kisch, 1984; Heyen *et al.*, 1982) and for the CO_2-N_2 system (Darimont & Heyen, 1988) have limited ranges of application and are

0935-1221/94/0006-0753 $ 4.75

inaccurate in some parts. Therefore, it was felt that more reliable thermodynamic models, with larger ranges of application and higher accuracy, are required in order to be in better agreement with fluid-inclusion data.

Earlier *vX* diagrams for the two binary systems were constructed by means of single models like cubic equations of state (Heyen, 1981; Peng & Robinson, 1976; Soave, 1972). However, it is not possible to build one cubic equation of state (EOS), that reproduces all thermodynamic properties of a fluid (Vidal, 1983). Therefore, instead of using only one EOS, two different thermodynamic models are successively applied as described by Thiéry *et al.* (1994). The first step is the calculation of the saturation pressure of a mixture of given composition and temperature from a cubic EOS. Subsequently, the molar volume is calculated from the calculated pressure with a model based on the corresponding-states principle (Prausnitz, 1969), the correlation developed by Lee & Kesler (1975). This method results in more accurate calculation of all parameters. Indeed, cubic EOS are efficient in modelling the *PTX* properties of phase equilibria in mixtures of non-polar molecules. On the other hand, the Lee-Kesler method is most successful when applied to the calculation of bulk properties such as the molar volume. In this way, *vX* diagrams have been published for the systems CO_2-CH_4 and CO_2-N_2 (Thiéry *et al.*, 1994). However, the results obtained for near-critical fluids are still poor as compositions in this range are inaccurate and the pressure is overestimated. Consequently, molar volumes in the critical and retrograde condensation regions are badly reproduced. This makes an improvement of the model for critical fluids necessary. Moreover, phase transitions involving a CO_2 solid phase (initial and final melting, partial homogenization and sublimation) are also indicative of *vX* properties of fluid inclusions (Van den Kerkhof, 1988). Modelling of these phase transitions is also addressed in the present paper. The previous models used by Heyen *et al.* (1982), Herskowitz & Kisch (1984), Darimont & Heyen (1988) are highly inaccurate in parts of the *vX* diagrams and the stability conditions of the univariant three-phase solid-liquid-gas assemblage are not well estimated. Modelling of the metastable liquid-liquid-gas assemblage, which has been recently described in fluid inclusions (Berdnikov, 1987; Van den Kerkhof *et al.*, 1993) has also been done with the same combined EOS.

Symbols

S	the CO_2 solid phase
F	the fluid phase
L	the liquid phase
L_1	the CH_4-rich liquid phase
L_2	the CO_2-rich liquid phase
G	the gas phase
S(LG)	the CO_2 solid phase in equilibrium with liquid and gas
L(SG)	the liquid phase in equilibrium with CO_2 solid and gas
G(SL)	the gas phase in equilibrium with CO_2 solid and liquid
LG(S)	the tie-line joining L(SG) and G(SL)
SG(L)	the tie-line joining S(LG) and G(SL)
SL(G)	the tie-line joining S(LG) and L(SG)
EOS	equation of state
SRK	the Soave-Redlich-Kwong equation of state
LK	the Lee-Kesler correlation
X	composition (mole fraction)
P	pressure (bar)
v	molar volume (cm^3/mol)
T	temperature (K)
k_{ij}	binary interaction parameter characteristic of components i and j used in the SRK EOS
δ_{ij}	binary interaction parameter in the LK correlation
ξ	a distance between non-critical conditions and critical conditions.

The topology of the CO_2-CH_4 and CO_2-N_2 systems

The main difference between the systems CO_2-CH_4 and CO_2-N_2 is due to the relative positions of the liquid-gas (L = G) critical and the univariant solid-liquid-gas (SLG) curves (Fig. 1). The critical curve is continuous between the two critical points of the pure components for the system CO_2-CH_4 (Fig. 1a), whereas it is discontinuous for the system CO_2-N_2 (Fig 1b). In the latter system, the critical curve is intersected twice by the univariant three-phase SLG curve, where solid phase is in equilibrium with critical fluid (SL = G). One of the intersection points (P point) is very close to the critical point of N_2, whereas the

intersection point at the high temperature side (Q point) has been located at XN_2 = 0.47 and T = -61°C (Van den Kerkhof, 1990). At temperatures not below -183°C, the solid phase is always pure CO_2. Solid solution between CO_2 and CH_4/N_2 does not occur. However, solid phases forming at lower temperatures involve solid solutions between CH_4 and N_2 (Omar, 1962). These solids are not considered here, since the purpose of this work is to model phase equilibria observed using liquid N_2 as cooling agent at temperatures above -182°C.

Recently, immiscibility of the metastable undercooled liquid has been observed in the CO_2-CH_4-N_2 system below -90°C (Berdnikov, 1987; Van den Kerkhof *et al.*, 1993, see below) and suggests that phase transitions in the systems CO_2-CH_4 and CO_2-N_2 may be more complex than first assumed (Kreglewski & Hall, 1983; Van Konynenburg & Scott, 1980). Based on a theoretical analysis of the van der Waals EOS, binary (*i* - *j*) systems show different topology in relation to the strength of molecular interactions (Van Konynenburg & Scott, 1980). In the case of strong attractive interactions between molecules *i* and *j*, mixing of the end-member fluids at low temperatures produces heat and, consequently, liquid-liquid immiscibility does not occur. Examples of such systems are CO_2 + ethanol and CO_2 + nitrobenzene, and have been classified by Van Konynenburg & Scott (1980) as type I. On the other hand, if interactions between *i* and *j* molecules are not very strong, heat must be furnished to mix the pure components, attractive forces are not strong enough to counteract the repulsive part of molecular interactions, and liquid-liquid immiscibility occurs at low temperatures. Moreover, if the critical temperature of one end-member component is much higher than the critical temperature of the other one (*i.e.*, $T_{c,j} > 2\ T_{c,i}$ for molecules of similar size), the attractive forces *(j - j)* are much stronger than attractive forces *(i - i)*. As shown by Van Konynenburg & Scott (1980), this must have also implications for the position of the liquid-gas critical curve relative to the liquid-liquid critical curve. If the difference between the critical temperatures of the end-members is not large, the liquid-gas critical curve does not intersect the liquid-liquid critical curve. These systems are classified as type II by Van Konynenburg & Scott (1980), *e.g.* the systems of CO_2—*n*-alkanes. If the difference between the critical temperatures of the end-member components is large, there is

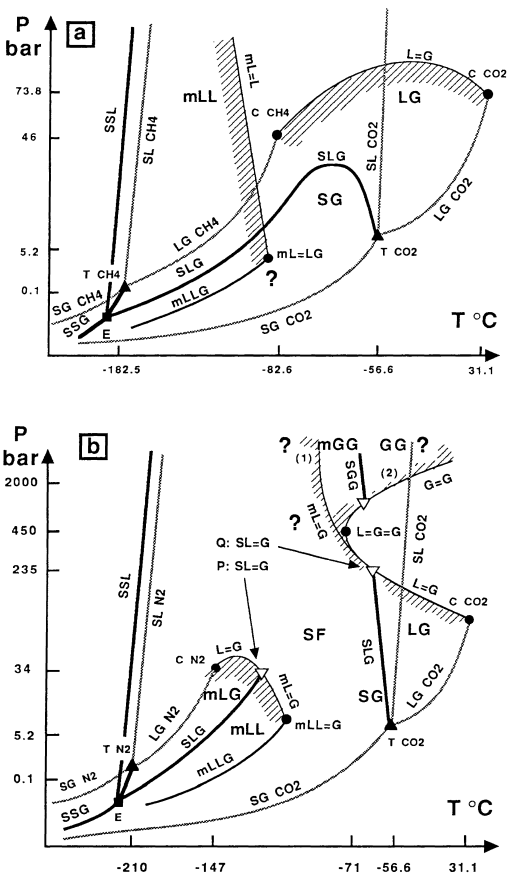

Fig. 1. Topology of the binary systems CO_2-CH_4 (Fig. 1a) and CO_2-N_2 (Fig. 1b) in *PT* diagrams. The pressure and temperature scales are arbitrary. Invariant points: eutectic point $S_{CH_4}/N_2S_{CO_2}LG$ (E, filled square), triple points (T, filled triangles), L = G critical points for pure fluids (C, filled circles), three-phase critical end-points (empty circles), intersection points of a critical curve with the SLG curve (empty triangles). Univariant lines: two-phase assemblage for the pure end-members (gray lines), three-phase assemblage for the binary systems (thick solid lines), and critical curves (thin solid lines). The prefix "m" denotes metastable parts. Regions around the triple points T CH_4 and T N_2 have been considerably enlarged. The critical curves (L = L and L = G) delimit LL and LG immiscibility (shaded areas). Also indicated are the stability fields of liquid-liquid (LL), solid-gas (SG) and solid-fluid (SF) assemblages. The metastable L = G critical curves (mL = G) predicted by the SRK EOS and the Kreglewski & Hall model (1983) are sketched.

no continuous liquid-gas critical curve, metastable or not, joining the critical points of the pure components. Such systems are classified as type III, *e.g.* the system H_2O-CO_2. Kreglewski & Hall (1983) suggested from calculations with their EOS that the CO_2-CH_4 system would be type II and the CO_2-N_2 system type III. According to their calculations, liquid-liquid immiscibility for the CO_2-CH_4 system would occur below -80°C in the stability field of solid CO_2. Furthermore, for the CO_2-N_2 system, the metastable branch of the critical curve starting from the Q point would exhibit a temperature minimum and then, would run with increasing temperatures to very high pressures and delimit the field of so-called gas-gas immiscibility (Schneider, 1978). The temperature minimum of the critical curve is referred to as a "double critical" point (L = G = G), where the liquid-gas and gas-gas critical loci meet. Kreglewski & Hall (1983) estimated the temperature of the double critical point at -71°C, 450 bars, and approximately 40 cm^3/mole. Thus, gas-gas equilibria may occur in fluid inclusions of lowest molar volume and above -71°C, but they are assumed to be indistinguishable from "normal" LG equilibria. Moreover, gas-gas immiscibility would occur partly in the stability field of solid CO_2 (denoted mGG field in Fig. 1b). In this case, a second intersection point with the SLG curve should exist and the G = G critical curve should become stable again at higher temperatures and pressures. However, gas-gas immiscibility is not predicted with the SRK EOS. The L = G critical curve calculated by the SRK EOS steeply rises to high pressures with cooling and shows no double critical point. The reality of gas-gas immiscibility can be proved by experiment only. A series of high-pressure experiments has been started at the van der Waals Laboratory, Amsterdam (Schouten *et al.*, in prep.). The low temperature side of the L = G critical curve starts from the critical point of N_2, intersects the three-phase SLG curve at the P point, and should go on metastably up to an intersection point (mLL = G point in Fig. 1b) with the three-phase metastable LLG curve. The metastable extension of the L = G critical curve at low temperature (mL = G in Fig. 1b) has never been observed, but is important to consider in order to understand the transition from the type-II system CO_2-CH_4 to the type-III system CO_2-N_2. When N_2 is added to the CO_2-CH_4 system, the LL stability field extends progressively to higher temperatures. Then, the L = L critical curve intersects the L = G critical curve. From this step on, the system becomes a type-III system, as illustrated in Fig. 1b: the L = G curve splits into a low-temperature and a high-temperature parts. The low-temperature side ends at a critical end-point (LL = G) on the LLG curve; and the high-temperature part starts from the CO_2 critical point and rises to high pressures as an extension of the previous L = L curve.

The larger difference between the critical temperatures of pure components for the system CO_2-N_2 compared to CO_2-CH_4 has also implications for the partitioning of the components in liquid and gas, and for the phenomena of retrograde condensation. The partitioning of N_2 is much higher in the gas phase and much lower in the liquid phase than CH_4. The phenomenon of retrograde condensation is important for the understanding of the binary systems and for a proper interpretation of fluid inclusions. Retrograde condensation is a remarkable fluid phase behaviour in mixtures : by compressing a gas mixture at constant temperature, as expected, liquid condensates, but again it may disappear during further compression. In pure systems, the critical point is the highest temperature of liquid-gas coexistence, and therefore the highest possible homogenization temperature. The implication of retrograde condensation for fluid inclusions is that, contrary to pure fluids, mixtures of given composition may homogenize to gas at a higher temperature than the critical temperature of the mixture with the same composition. Retrograde condensation is very common for CO_2-N_2 fluid inclusions.

Phase equilibria modelling

Modelling of liquid-gas phase equilibria

Modelling of liquid-gas equilibria is carried out using the Soave-Redlich-Kwong (SRK) EOS (Soave, 1972), associated with the quadratic mixing rules (Vidal, 1978). As shown by Thiéry *et al.* (1994), such an EOS could be successfully applied to CH_4-CO_2-N_2 fluids except in the critical and retrograde condensation regions. The pressure is strongly overestimated in the critical region (up to 50 bars for the CO_2-N_2 system, at -30°C) and the CO_2 content at the critical point

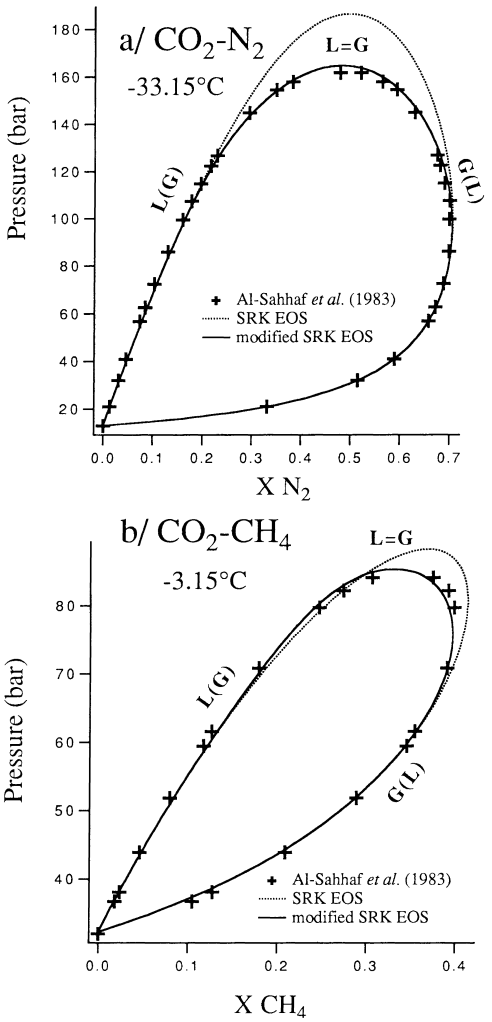

Fig. 2. *PX* isothermal LG immiscibility curves of the binary systems. (a) CO_2-N_2, (b) CO_2-CH_4. Experimental data of Al-Sahhaf *et al.* (1983).

is always underestimated (up to 10 percent), as shown in Fig. 2. Therefore, an improvement of the EOS is necessary for any quantitative use.

As shown by Huron *et al.* (1978), the SRK EOS is able to predict liquid-gas equilibria in the critical region for binary mixtures of CO_2 and *n*-alkanes, if binary interaction parameters (BIP) are determined from experimental data along the critical lines. However, these critical BIP are not suitable outside the critical region. Therefore, BIP should be expressed as a function of some characteristic distance between non critical and critical conditions for using the SRK EOS over the whole range of conditions.

$$k_{a,ij} = \xi k^{c}_{a,ij} + (1-\xi)k^{nc}_{a,ij} \quad (1a)$$

$$k_{b,ij} = \xi k^{c}_{b,ij} + (1-\xi)k^{nc}_{b,ij} \quad (1b)$$

where superscripts *nc* and *c* denote non-critical and critical conditions respectively. ξ is an interpolation parameter ranging between 0 (non-critical state) and 1 (critical state); $k^{nc}_{a,ij}$, $k^{nc}_{b,ij}$, $k^{c}_{a,ij}$, and $k^{c}_{b,ij}$ are BIP, determined independently by fitting the EOS with experimental data. Determination of ξ can be done by making use of the fact that molar volumes of the gas and liquid phases become almost equal for the critical conditions. Accordingly, ξ is expressed as function of v_r , the ratio of the molar volume of the gas (v_G) the molar volume of the coexistent liquid (v_L):

$$v_r = \frac{v_G}{v_L} \quad (2)$$

where v_G and v_L are calculated with the classical SRK EOS (ξ = 0).

A threshold function has been used to describe the dependence of the ξ parameter to v_r:

$$\xi = \exp\left(-\frac{1}{2}(1.05 - v_r)^2\right) \text{ for } v_r > 1.05 \quad (3a)$$

$$\xi = 1.0 \text{ for } v_r < 1.05 \quad (3b)$$

Best-fitting k^{nc}_{ij} BIP have been determined in a previous study in the non-critical region (Thiéry *et al.*, 1994) from experimental data of the binary systems CH_4-N_2, CO_2-N_2 and CO_2-CH_4 (Al-Sahhaf *et al.*, 1983; Arai *et al.*, 1971; Chang & Lu, 1967; Cines *et al.*, 1953; Davalos *et al.*, 1976; Hwang *et al.*, 1976; Kidnay *et al.*, 1985; Mraw *et al.*, 1978; Muirbrook & Prausnitz, 1965; Neumann & Walch, 1968; Parrish & Hiza, 1974; Somait & Kidnay, 1978; Stryjek *et al.*, 1974; Zenner & Dana, 1963). The $k^{nc}_{b,ij}$ values have been set to zero, and the $k^{nc}_{a,ij}$ values are temperature independent (Table 1).

Optimum k^{c}_{ij} BIP have been determined along the critical locus curve for the CO_2-N_2 and the CO_2-CH_4 systems from available experimental data (Al-Sahhaf *et al.*, 1983; Arai *et al.*, 1971; Davalos *et al.*, 1976; Krichevskii *et al.*, 1962; Mraw *et al.*, 1978; Muirbrook & Prausnitz, 1965; Zenner & Dana, 1963). Slight discrepancies have been recognized between the data of Arai *et al.* (1971) and other data (Krichevskii *et al.*, 1962; Zenner & Dana, 1963). The CO_2 mole fraction of the critical points given by Arai *et al.* (1971) is overestimated by 2-3 percent. Arai's experimental data of critical points were obtained by

Table 1 : parameters used for the calculations of BIP.

i – j	$CO_2 - CH_4$	$CO_2 - N_2$	$CH_4 - N_2$
$k^{nc}_{a,ij}$	0.1	-0.035	0.03
$k^{nc}_{b,ij}$	0.0	0.0	0.0
$k^{cc}_{a,ij}$	0.06	-0.13	0.03
$k^{cc}_{b,ij}$	-0.10	-0.08	0.0
$T_{a,ij}$ (K)	255	235	-
$\sigma_{a,ij}$ (K)	15	15	-
$T_{b,ij}$ (K)	255	235	-
$\sigma_{b,ij}$ (K)	5	15	-

extrapolation of their bubble and dew points measurements, but as explained below, their method is not accurate enough for measuring dew points. Consequently, the CO_2 contents of their dew point data are overestimated when compared to other published experimental data. For this reason Arai's experimental data of critical points have not been taken into account for the fitting of k^c_{ij} BIP along the critical curve. Critical data obtained from fluid inclusion data could be a help for the construction of the critical curve, but most data are not accurate enough for the present calculations. Diamond (1986) noticed similar discrepancies by comparing Arai's data of critical points with his data from CO_2-N_2 fluid inclusions, showing critical homogenization, for which both Raman-spectroscopic and microthermometric analyses are available. However, microthermometry and revised Raman data of Van den Kerkhof (1988) for experimentally produced fluid inclusions give two additional critical loci at 2°C (XN_2 = 0.25) and at -57°C (XN_2 = 0.44). These data show somewhat higher CO_2 contents compared to Arai *et al.* (1971).

Better agreement of the model with experimental data of critical loci is achieved when non-zero values for the $k^c_{b,ij}$ parameters are taken. Moreover, $k^c_{a,ij}$ and $k^c_{b,ij}$ BIP are temperature-dependent and strongly correlated. At low temperatures, $k^c_{a,ij}$ and $k^c_{b,ij}$ values tend to converge to the values of $k^{nc}_{a,ij}$ and $k^{nc}_{b,ij}$. Towards the critical temperature of CO_2, $k^c_{a,ij}$ and $k^c_{b,ij}$ BIP become constant , denoted as $k^{cc}_{a,ij}$ and $k^{cc}_{b,ij}$ respectively. By taking into account these considerations, the following empirical relations for $k^c_{a,ij}$ and $k^c_{b,ij}$ BIP are proposed:

$$k^c_{a,ij} = \frac{k^{cc}_{a,ij} + k^{nc}_{a,ij}}{2} + \frac{k^{cc}_{a,ij} - k^{nc}_{a,ij}}{2} \tanh\left(\frac{T - T_{a,ij}}{\sigma_{a,ij}}\right) \quad (4a)$$

$$k^c_{b,ij} = \frac{k^{cc}_{b,ij} + k^{nc}_{b,ij}}{2} + \frac{k^{cc}_{b,ij} - k^{nc}_{b,ij}}{2} \tanh\left(\frac{T - T_{b,ij}}{\sigma_{b,ij}}\right) \quad (4b)$$

Values of parameters of these relations are given in Table 1.

This model has been used for gas-liquid equilibria calculations with the Asselineau *et al.*

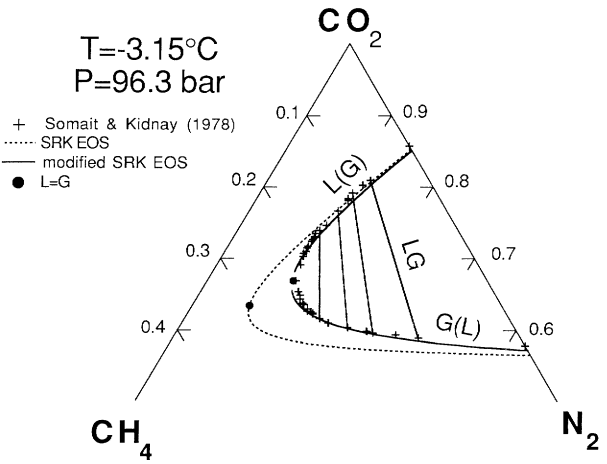

Fig. 3. Isothermal and isobaric LG immiscibility curve in the ternary CO_2-CH_4-N_2 system: comparison of the models with experimental data.

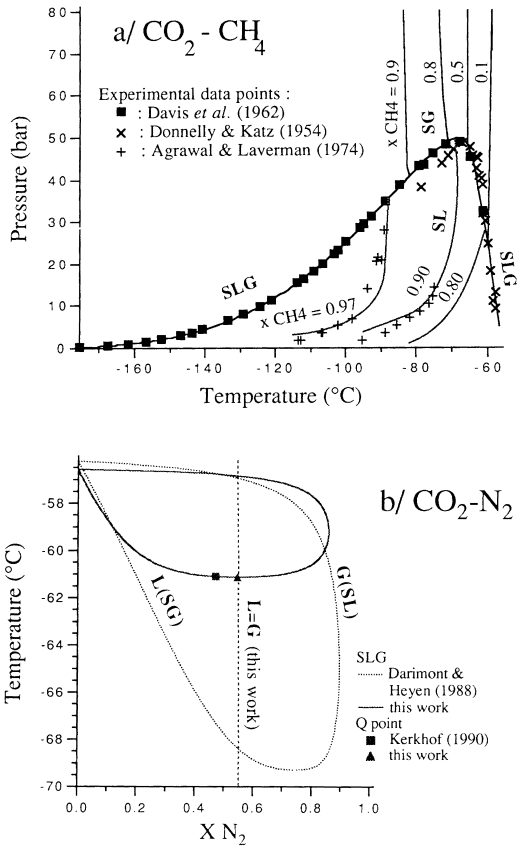

Fig. 4. SLG stability curve calculated with the modified SRK EOS
(a) *PT* diagram in the CO_2-CH_4 system. The SLG curve delimits the SL stability field from the SG stability region. SL isopleths and SG isopleths have been calculated for different methane compositions.
(b) *TX* diagram in the CO_2-N_2 system. The SLG stability area is calculated with the Heyen EOS (dotted line) and with our model (solid line). The L = G critical curve calculated by our model is represented by the dashed line. The Q point obtained with our model is in fair agreement with the estimation of Van den Kerkhof (1990), using synthetic fluid inclusions.

(1979) algorithm. The improvements for the CO_2-N_2 and the CO_2-CH_4 systems are shown in Fig. 2. In contrast to the classical SRK EOS, the pressure is no more overestimated and the compositions in the critical and retrograde condensation regions are reproduced better. Cubic EOS can be used for liquid-liquid and liquid-liquid-gas immiscibility calculations in "simple" cases (for example, methane—*n*-hexane mixture, Vidal, 1984) and have also been used for the systems investigated in this work. The model has been also applied to the ternary system. A comparison between the predicted values and the experimental data of Somait *et al.* (1978) shows fairly good agreement (Fig. 3).

Modelling of phase equilibria involving a CO_2 solid phase

In order to apply the SRK EOS to SLG, SL and SG equilibria, an expression of the fugacity of CO_2 in the CO_2 solid phase must be derived as a function of pressure and temperature. Smoothed pressure-temperature data of the sublimation curve of the CO_2 system, reported by Angus *et al.* (1976) have been converted in fugacity values with the SRK EOS. Obtained fugacity $f^s_{CO_2}$ values have been fitted by the following expression :

$$\ln f^s_{CO_2} = 13.08053 - 0.0047478\ (T - 216.58) - 3250.44\left(\frac{1}{T} - \frac{1}{216.58}\right) + \frac{Pv_s}{RT} \quad (5)$$

where v_s denotes the molar volume of CO_2 solid phase (v_s = 28.7552 cm³/mole, Angus *et al.*, 1976). Contrary to the model developed by Heyen (Darimont & Heyen, 1988; Heyen *et al.*, 1982), the pressure dependence of $f^s_{CO_2}$ is taken into account as high pressures can be reached (up to 200 bars) for the CO_2-N_2 system .

The SRK EOS predicts the saturation curve of pure CO_2 with 1-2 % accuracy (Thiéry *et al.*, 1994); but in the vicinity of the CO_2 triple point (T = 216.58 K = -56.57°C, P = 5.185 bars), higher accuracy of the SRK EOS is required. Otherwise, like the Heyen EOS, the temperature of the triple point would be overestimated by a few tenths of a degree. Therefore, the dependence of the a_{CO_2} parameter with temperature has been modified as follows :

for $T > 216.58$ K

$$a_{CO_2}(T) = 0.999404\ a^{Soave}_{CO_2}(T) \exp\left(-10\,\frac{T-216.58}{216.58}\right) \quad (6a)$$

for $T < 216.58$ K

$$a_{CO_2}(T) = 0.999404\ a^{Soave}_{CO_2}(T) \quad (6b)$$

where $a^{Soave}_{CO_2}(T)$ is the a_{CO_2} parameter calculated by the relation given by Soave (1972).

The modification does not alter the quality of the model for predicting liquid-gas equilibria.

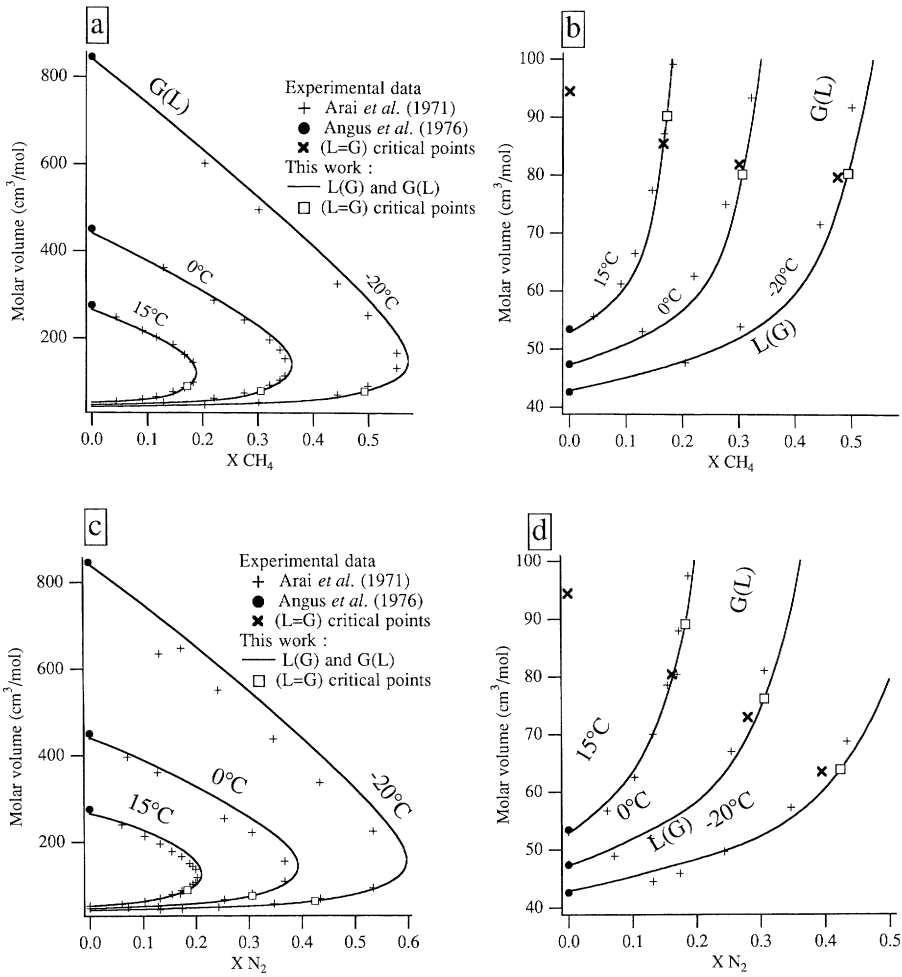

Fig. 5. Projections of the LG isotherms in *vX* diagrams, calculated at -20°C, 0°C and 15°C including the experimental data (Angus *et al.*, 1976; Arai *et al.*, 1971). (a and b) CO_2-CH_4 system; (c and d) CO_2-N_2 system.

Results given by our model for SLG and SG are in good agreement with experimental data (Agrawal & Laverman, 1974; Davis *et al.*, 1962; Donnelly & Katz, 1954) for the CO_2-CH_4 system (Fig. 4a). For the CO_2-N_2 system, experimental SLG data are not available. However, Van den Kerkhof (1990) determined the intersection point of the critical and solid-liquid-gas curves (SL = G) at a temperature of -61.2°C and XN_2 around 0.47, using synthetic fluid inclusions. These values are in good agreement with our model (-61.1°C, XN_2 = 0.55) as shown in a *TX* diagram (Fig. 4b). This temperature must also correspond to the lowest possible CO_2 melting temperature in the system CO_2-N_2 and could be confirmed by the evaluation of microthermometry data. In comparison, the Heyen EOS (Darimont & Heyen, 1988) produces a lower minimum CO_2 melting temperature of -70°C.

Molar volume modelling

The Lee-Kesler (LK) correlation (Lee & Kesler, 1975) has been used for calculating the molar volume of fluids from their *PTX* properties. However, the original Lee-Kesler mixing

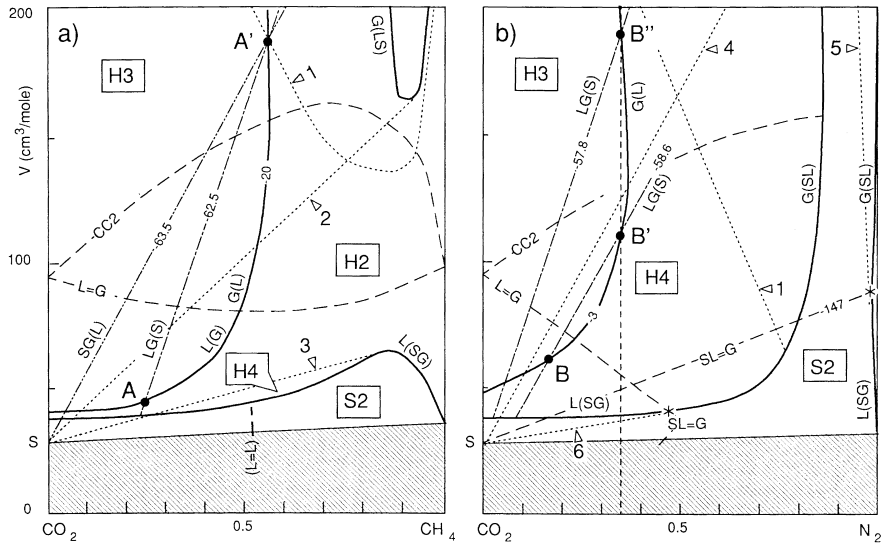

Fig. 6. The use of *vX* diagrams for the determination of molar volume and composition from microthermotric data. (a) the system CO_2-CH_4, (b) the system CO_2-N_2.
Thick solid line : L(SG) and G(SL) curves. Inclusions plotting in the shaded area are classified as "S-type" (mostly S2) and may show metastable LG homogenization below melting. Inclusions plotting outside the shaded area are classified as "H-type". Inclusions plotting below the critical curve (L = G) homogenize to liquid, above the critical curve to gas. Inclusions between the curve denoted as CC2 (second-order critical curve) and L = G show (LG → G) homogenization to gas at higher temperature than critical for given composition as a consequence of retrograde condensation. Most common phase transition sequences are indicated by H2, H3, H4 and S2 (see text). The type boundaries are given by line 2 (H2-H3), line 3 (H2-H4), and line 4 (H3-H4). Line 1 (in both diagrams) indicates fill degrees of 10 % liquid: the liquid phase in inclusions plotting above these lines can normally not be observed in fluid inclusions due to optical restrictions. Similarly, line 5 indicates fill degrees of 1 % for SG equilibria: the solid phase cannot be observed above this line. Inclusions plotting left of line 6 show complex "S-type" behaviour (S1, S2 and S3). Line signatures for the phase transitions are the following: thin solid lines = homogenization (LG → L or G); dashed-dotted lines = final melting (SLG → LG); dashed-double dotted lines = initial melting (SG → SLG), bubble nucleation (SL → SLG) or partial homogenization (SLG → SG or SLG → SL).
Following inclusions are given as an example for the system CO_2-CH_4: (A) Type H2: *Tm* = -62.5°C, *Th(L)* = -20°C; (A') Type H3: the same *Th* and *Tm* as inclusion A, but LG homogenization to the gas phase and initial melting can be observed at -63.5°C. In the system CO_2-N_2: (B) Type H4: *Tm* = -58.6°C and *Th(L)* = -3°C. As B plots above the SL = G line, partial homogenization will be to the gas phase (SLG → SG) and expected around -153°C (line not shown). Temperature difference between initial and final melting is very small and lines for *Ti* are omitted here; (B') Type H4: Inclusion showing the same *Th* and *Tm* as inclusion B, but homogenization to the gas phase; (B") Type H3: inclusion showing homogenization to gas phase at the same temperature as for inclusion B', but melting temperature is higher (-57.8°C).

rules have been slightly modified by introducing a new interaction parameter δ_{ij} in the calculation of the pseudo-critical temperature of the mixture (Thiéry *et al.*, 1994). This modification was suggested in order to improve the accuracy of molar volumes calculations in the critical region.Values of δ_{ij} are the following : δ CO_2 - N_2 = -0.08, δ CO_2 - CH_4 = 0.02. As shown by Thiéry *et al.* (1994), the Lee-Kesler correlation gives accurate results for the molar volumes of saturated liquids and vapours of pure CO_2, CH_4 and N_2 (Angus *et al.*, 1976, 1978, 1979), except for conditions very near the critical point. For the binary CO_2-CH_4 and CO_2-N_2 systems, the only available *PvTX* data are those of Arai *et al.* (1971). Fair agreement is obtained between the present model and the experimental data (Arai *et al.*, 1971) of molar volumes of saturated liquids (Fig. 5a, 5b, 5c and 5d), but the model seems to overestimate the molar volumes of saturated vapour. As it is not

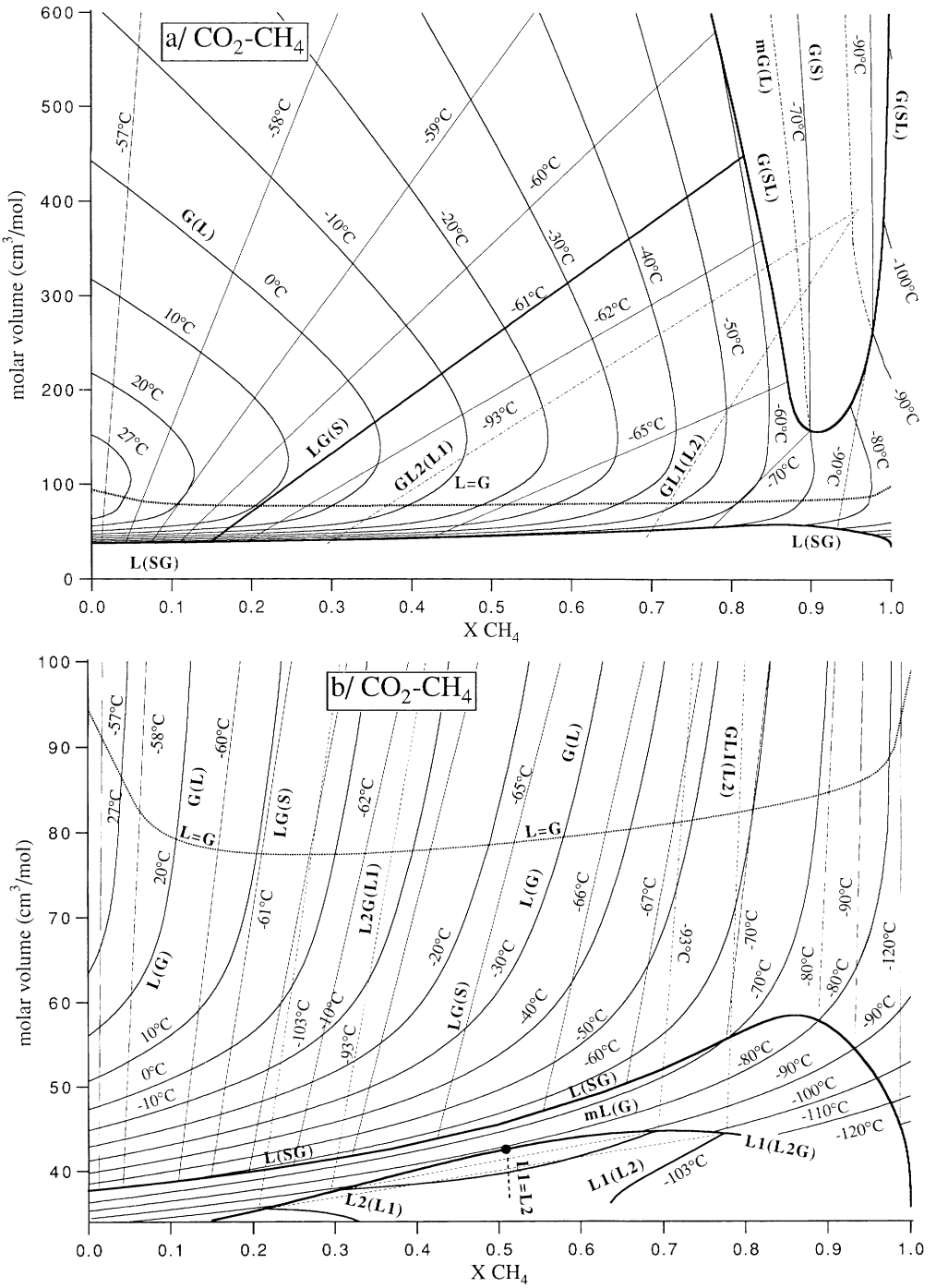

Fig. 7. *vX* diagrams calculated for the CO_2-CH_4 system, (a) for high molar volumes (v < 600°Ccm^3/mole), (b) for intermediate molar volumes (v < 100cm^3/mole), (c) for low molar volumes (v < 70cm^3/mole). The L = G critical curves have to be smoothed, as values given by our model show local maxima and minima, which are not realistic. It is worth noting (see Fig. 5b) that molar volumes of critical fluids are very sensible to all parameters *PTX*. Metastable liquid-liquid and liquid-liquid-gas phase transitions are shown in Fig. 7b and will be explained further.

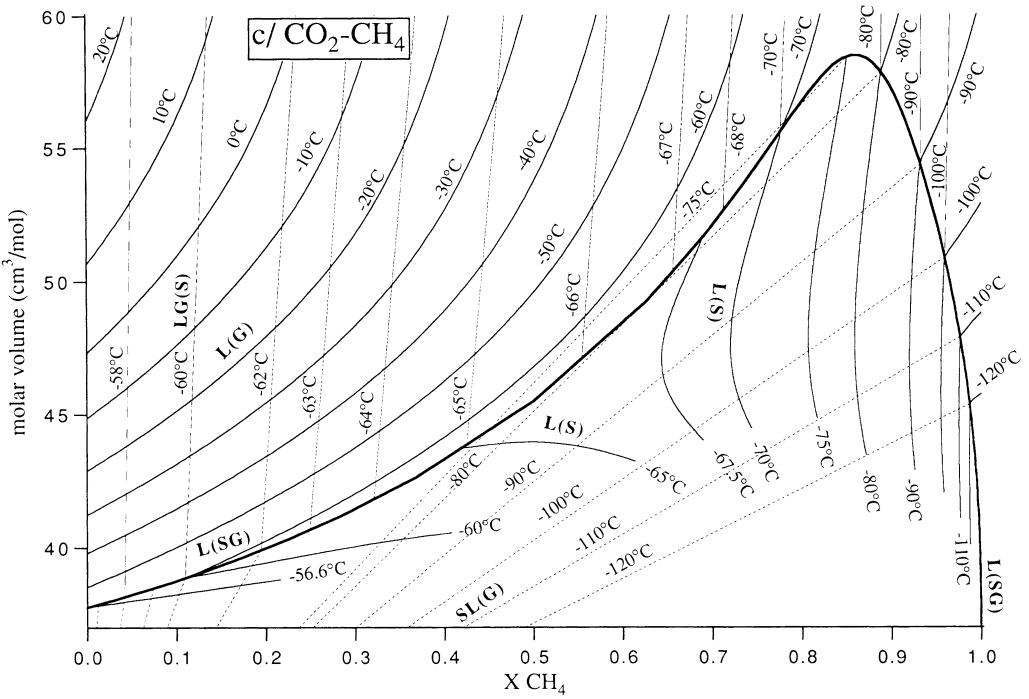

Fig. 7 (continued)

possible to compare with other experimental data, it is useful to look in more detail at the experimental method. Arai *et al.* (1971) used the dew and bubble point apparatus with a glass equilibrium cell, in which a gaseous mixture of known composition was compressed through the dew point and the bubble point by adding mercury to a fixed volume. Dew and bubble points were observed visually and also determined by discontinuities of pressure and volume data. This method is accurate for determining bubble points, as the disappearance of the last bubble in the cell is visible and marked by a rapid change of the pressure-volume slope. However, for the dew points, the change of the slope is much less evident, and it is difficult to observe the disappearance of the thin film of liquid on the surface of the equilibrium cell. Therefore, at the time the dew point measurements were done, a small amount of liquid may still have been present. This must be the reason why measurements of the CO_2 composition of the dew points of Arai *et al.* (1971) are systematically overestimated by 2-4 %, when compared to other experimental data (Al-Sahhaf *et al.*, 1983; Davalos *et al.*, 1976; Muirbrook & Prausnitz, 1965; Somait & Kidnay, 1978; Zenner & Dana, 1963). Consequently, molar volumes of the gas phase given by Arai *et al.* (1971) are assumed to be underestimated by up to 30 cm^3/mole.

Application to fluid inclusions

The *vX* diagrams

The determination of molar volume and composition is one of the principal steps in fluid-inclusion studies. *vX* phase diagrams are most useful for the interpretation of microthermometry and Raman analysis of binary fluid inclusions. The use of *vX* diagrams for the determination of molar volume and composition is illustrated in Fig. 6. Calculated *vX* diagrams are given for the CO_2-CH_4 system in Fig. 7 and for the CO_2-N_2 system in Fig. 8. Fluid inclusions behave as constant molar volume and composition systems. Consequently, a fluid inclusion is represented as a fixed point in the relevant *vX* diagram.

The stability curve of a SLG phase assemblage

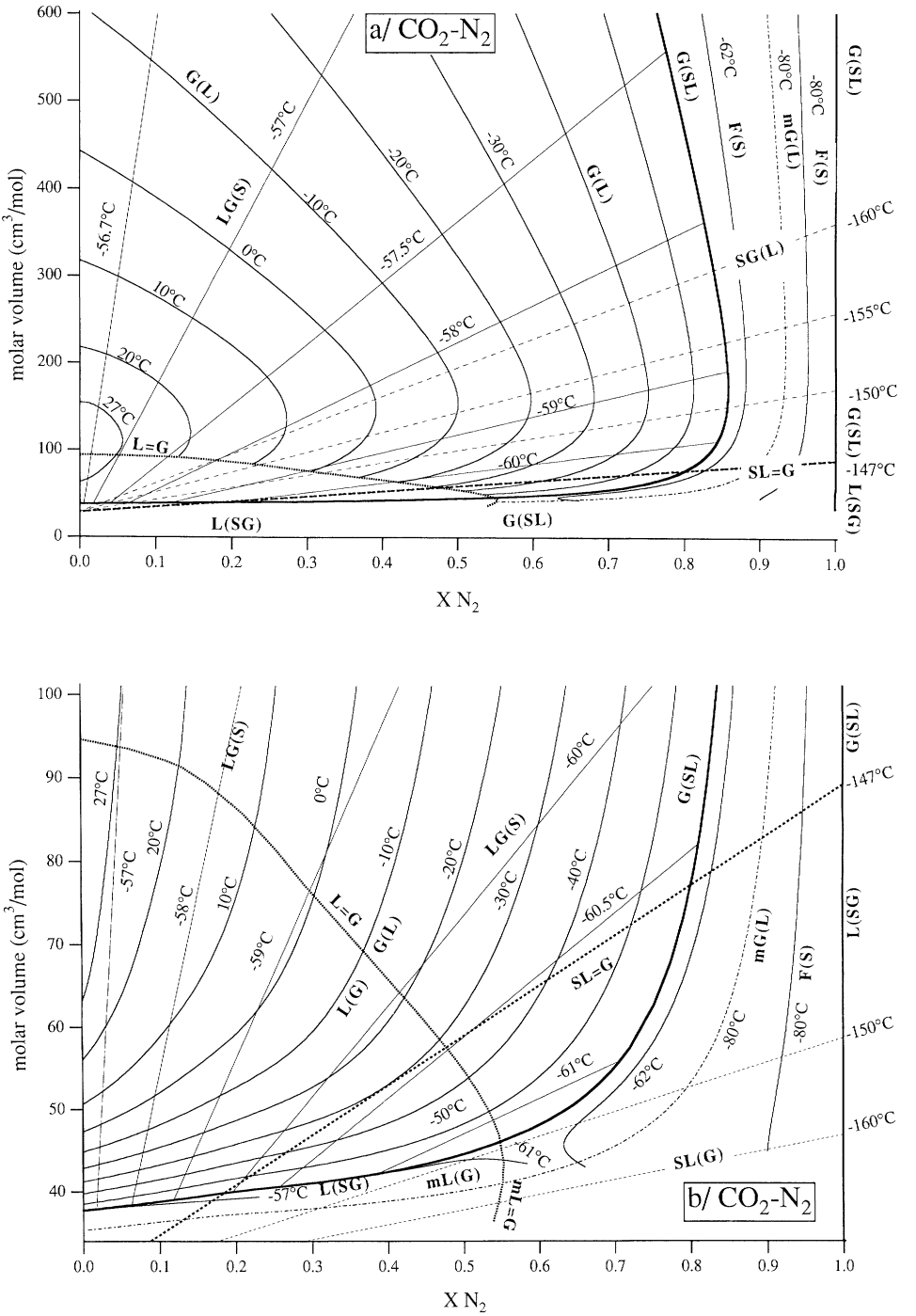

Fig. 8. *vX* diagrams calculated for the CO_2-N_2 system, (a) for high molar volumes (v < 600cm^3/mole), (b) for low molar volumes (v < 100cm^3/mole).

(*cf.* Fig. 1 and 4) splits into three parts in a *vX* diagram: the L(SG) curve, the G(SL) curve and the S point. As shown by the phase rule, a three-phase association in a binary system is invariant for a given temperature, *i.e.*, all intensive properties (and, thus *vX* properties) of the coexisting phases are fixed. Hence, a fluid inclusion containing a SLG assemblage is defined in a *vX* diagram by a point located inside the triangle shaped by the three apices describing the *vX* properties of the liquid, gas and solid phases. The relative position of the fluid inclusion point inside this triangle is a function of the volume percentages of the coexisting phases. When one of the three phases disappears on changing temperature, the fluid inclusion point must be located on the tie-line connecting the two remaining phases. For example, if we observe a phase transition like SLG $\rightarrow$ LG (final melting) at temperature T_m, the fluid inclusion point must plot on the tie-line joining the points, which define the *vX* properties of the liquid and gas phases, *i.e.* L(SG, $T = T_m$) and G(SL, $T = T_m$) respectively, at the disappearance of the last CO_2 crystal. The same rule can be similarly applied for other phase transition types like initial melting (SG $\rightarrow$ SLG, SL $\rightarrow$ SLG) and partial homogenization (SLG $\rightarrow$ SG, SLG $\rightarrow$ SL).

The variance of a two-phase assemblage for a given temperature is equal to one. The intensive properties of both phases are not defined, unless one extra parameter is given. In other words, the *vX* properties of each of the coexisting phases are represented by a curve at a given temperature in a *vX* diagram. This is the case for LG assemblages, which are described for any temperature by a set of tie-lines connecting two *vX* points on L(G) and G(L) curves. For SL and SG assemblages, one isothermal curves degenerates into a point, as the *vX* properties of the CO_2 solid phase are fixed. When one of the two coexisting phases disappears, the fluid inclusion point must be situated on the curve describing the *vX* properties of the remaining phase at that temperature. For example, for the phase transition LG $\rightarrow$ L at temperature T_h, the fluid inclusion point necessarily plots on the isothermal L(G, $T = T_h$) curve, for LG $\rightarrow$ G on the isothermal G(L, $T = T_h$) curve. G(L) isotherms exhibit a minimum in CO_2 concentration; this point is called "critical point of the second order" (Van den Kerkhof, 1988) or "cricondentherm" (Asselineau *et al.*, 1979; King, 1969). LG assemblages with gas homogenizations between the critical point and the "critical point of the second order" are typified by "retrograde condensation". The implication of retrograde condensation for fluid inclusions is that for given compositions, homogenizations (to gas) are observed at higher temperatures than the critical temperature of the same isopleth (Fig. 6). For example, CO_2-N_2 inclusions with 25% N_2, homogenize critically at around 7°C, but homogenizations to gas can be found as high as about 12°C (Van den Kerkhof, 1988). This effect is particularly valid for the system CO_2-N_2, where the field of retrograde condensation extends to lower molar volumes. Two fluid inclusions of the same composition and the same homogenization temperature to gas may have different molar volumes and can be distinguished by different melting temperatures. For example, CO_2-N_2 fluid inclusion with 25 % N_2 and homogenizing at 10°C in the retrograde condensation field would show melting of CO_2 at -58.4°C, whereas CO_2 solid would melt at -57.6°C for fluid inclusions homogenizing outside the retrograde condensation field.

The molar volume and compositions of fluid inclusions entirely determines the sequence of phase transitions observed during cooling runs. Van den Kerkhof (1988, 1990) proposed to distinguish between two main types of phase behaviour in CO_2-CH_4-N_2 inclusions, namely inclusions showing LG-homogenization ("H-type") and inclusions showing SG or SL-homogenization ("S-type", sublimation) as the final phase transition. The number of possible phase transitions may vary from 1 to 4 for both types, but the order of phase transitions is always the same *i.e.* SLG $\rightarrow$ (SL or SG) $\rightarrow$ SLG $\rightarrow$ LG $\rightarrow$ (L or G) for "H-type" inclusions and SLG $\rightarrow$ SL $\rightarrow$ SLG $\rightarrow$ (SL or SG) $\rightarrow$ (L or G) for "S-type" inclusions. Type and number of phase transitions are indicative for *vX* properties of fluid inclusions. All phase transitions can be read from the present diagrams. For example for a "H-type" inclusion showing four phase transitions (H4) the tie-lines for partial homogenization (SL $\rightarrow$ SLG), initial melting (SLG $\rightarrow$ SL), final melting (SLG $\rightarrow$ LG) and the homogenization-temperature L(G) isotherm should intersect in one point in the *vX* diagram. The *vX* properties of fluid inclusions can be obtained from two phase transitions, which are not necessarily homogenization and final melting only. Partial homogenization (SLG $\rightarrow$ SL or SLG $\rightarrow$ SG) may give more accurate interpretations *e.g.* if melting temperatures are difficult to measure like in CO_2-N_2 mixtures.

Contrary to the system CO_2-CH_4, the range of CO_2 melting temperatures for the system CO_2-N_2 (between -56.6 and -61°C) is small and the difference between initial (SLG → SG or SLG → SL) and final melting (SLG → LG) is only on the order of tenth of a degree. Therefore highest accuracy of melting temperature measurements is required in order to determine *vX* properties from microthermometry data only (without additional Raman analysis). For inclusions containing additional water this will be difficult and sometimes impossible as the gas phase will be enriched in CH_4 and N_2 by the formation of clathrate hydrates at low temperatures (Seitz *et al.*, 1987). On the other hand, clathrate hydrates in fluid inclusions may show a stability maximum during cooling (Murphy & Roberts, in press) and decompose on cooling to very low temperatures (and at low pressures).

The evolution of degree of fill of fluid inclusions homogenizing at the same temperature

Our model has been applied to simulate the variation of the degree of fill of CO_2-CH_4 fluid inclusions. An example is given for fluid inclusions homogenizing either to liquid or to gas at -3.15°C and with compositions ranging from pure CO_2 up to critical CO_2-CH_4 mixture (Fig. 9). It can be seen that the variation of the degree of fill is small at temperatures well below the homogenization point. Retrograde condensation behaviour can be diagnosed for fluid inclusions with significant higher degrees of liquid fill than fluid inclusions of the same composition with much lower degrees of fill. For example, two CO_2-CH_4 fluid inclusions with the same composition of 34 % CH_4 and the same T_h(G) at -3.15°C have strongly different fill degrees (around the melting point) of 0.43 and 0.11 volume percent of liquid. In practice, homogenization to gas can be observed only when degrees of fill are higher than 0.1. That means that observed gas homogenizations normally present fluids typified by "retrograde condensation", as gas homogenizations of "normal" fluids can only be observed with difficulty.

The liquid-liquid-gas immiscibility

In the system CO_2-CH_4-N_2 immiscibility of the liquid phase in fluid inclusions has been recently observed for the metastable, undercooled liquid and shows evidence for the existence of a liquid immiscibility gap (L_1L_2) besides LG immiscibility (G = CH_4-N_2-rich gas; L_2 = CO_2-rich liquid; L_1 = CH_4-rich liquid) (Berdnikov, 1987; Van den Kerkhof *et al.*, 1993). Metastable phase transitions in fluid inclusions (Fig. 10) occur on cooling below melting, but at higher temperatures than solid nucleation, normally between -110 and -80°C. Just before the freezing point, but always below -92°C, liquid immiscibility is evident from the L_1L_2G or L_1L_2 phase assemblages. In the case of no liquid immiscibility, L_1G persists down to the freezing point. Subsequent warming results in a combination of the following metastable phase transitions (Fig. 10a): (1) liquid homogenization at -95 ± 2°C by the disappearance of the outer meniscus ($L_1L_2G \rightarrow L_1G$); (2) simple liquid homogenization ($L_1L_2 \rightarrow L$); (3) rare L_1G-homogenization by first disappearance of the inner meniscus ($L_1L_2G \rightarrow L_1L_2$) and (4) liquid-gas homogenization ($L_1G \rightarrow L_1$). Van den Kerkhof *et al.* (1993) observed combined phase transitions (1) + (4), (2), and (3) + (2) for inclusions of about the same composition and re-

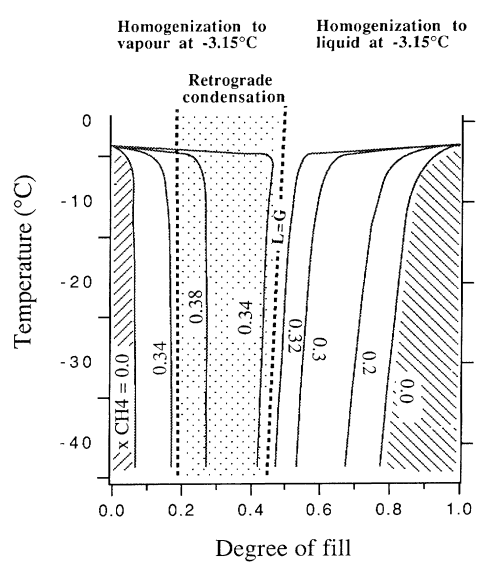

Fig. 9. Evolution of the volume fraction of the liquid upon cooling, for CO_2-CH_4 fluid inclusions homogenizing at -3.15°C either to liquid or to gas, and for composition ranging from pure CO_2 up to critical CO_2-CH_4 composition. Note difference in degree of fill for two fluids homogenizing to gas at -3.15°C with the same composition, but different molar volume.

spective lower molar volume. Simple liquid homogenization is optically similar to LG → G homogenization. The L_1L_2G phase assemblage can be calculated for the binary system CO_2-CH_4 with our EOS. However, as liquid-liquid-gas phase assemblages have never been observed in binary CO_2-CH_4 fluid inclusions, this phenomenom was believed to be more common for ternary CO_2-CH_4-N_2 fluids. Therefore, our model has been applied in order to investigate the *vTx* conditions of the liquid-liquid-gas phase assemblages also for ternary mixtures. Fluid inclusion data and calculated liquid-liquid-gas isotherms at -103°C, -93°C and -83°C are shown in a ternary CO_2-CH_4-N_2 diagram (Fig. 11). It can be seen that metastable liquid-liquid-gas immiscibility occurs below -83°C. The immiscibility area strongly expands to lower temperatures and also covers the CO_2-CH_4 system below -90°C. Moreover, at a given temperature and with increasing N_2 content, the CH_4-rich liquid (L_1) curve meets the gas curve at a critical point (L_2L_1 = G), and a continuous line joins the (L_1 = L_2) critical point to the (L = G) critical point of the CO_2-N_2 mixture.

Discussion

The present phase diagrams show differences with the existing diagrams which not only affect

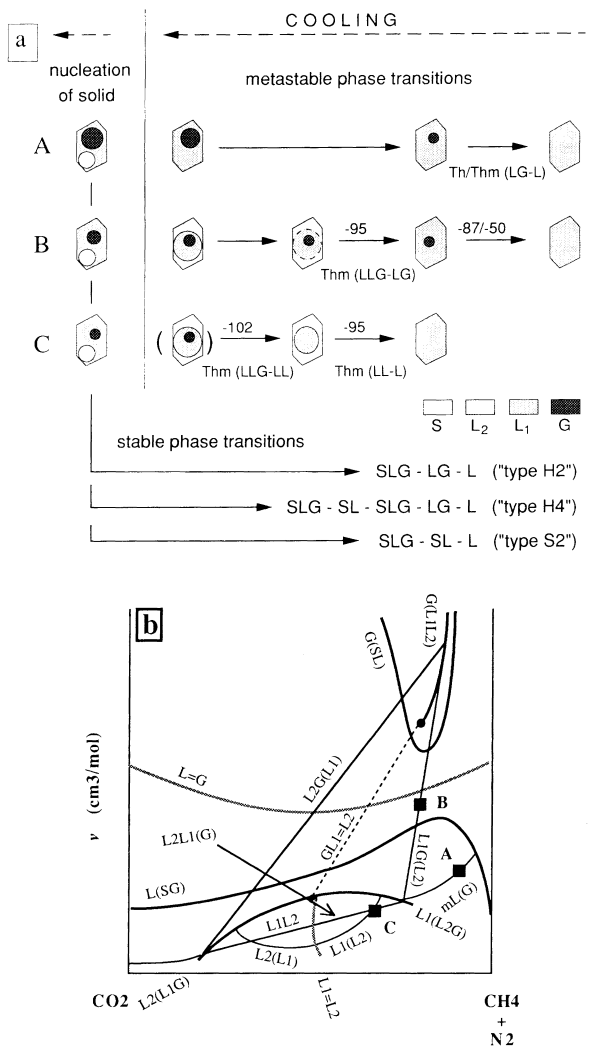

Fig. 10. (a) Phase transitions with liquid immiscibility observed in CO_2-CH_4-N_2 fluid inclusions (Van den Kerkhof *et al.*, 1993). Immiscibilities of the undercooled liquid (at higher temperature than solid nucleation) results in (A) L_1G, (B) L_1L_2G or (C) L_1L_2 phase assemblages. On subsequent warming, LL homogenization is observed around -95°C, before LG homogenization, or more rarely (v < 42 cm^3/mole) LG homogenization before LL homogenization. Phase transitions sequences observed on warming the "frozen" inclusions (SLG) are typified as H2, H4, or S2 (see text).(b) Interpretations of metastable phase transitions in a *vX* diagram for a pseudo-binary mixture CO_2-(CH_4 ± N_2). Thick solid lines : univariant three-phase curves : L(SG), G(SL), $L_1(L_2G)$, $L_2(L_1G)$ and $G(L_1L_2)$. Thick gray lines : critical curves L_1 = L_2 and L = G. Thin solid lines : metastable isotherm mL(G) at -102°C, isotherms $L_2(L_1)$ and $L_1(L_2)$ at -95°C. Thin solid lines : tie-lines L2G(L1), L1G(L2) and L1L2(G) at -102°C. Dotted line : the tie-line $GL_1 = L_2$ connecting the gas and the liquid (filled circles) at the critical end-point $GL_1 = L_2$. Filled squares : relative positions of fluids inclusions A, B and C.

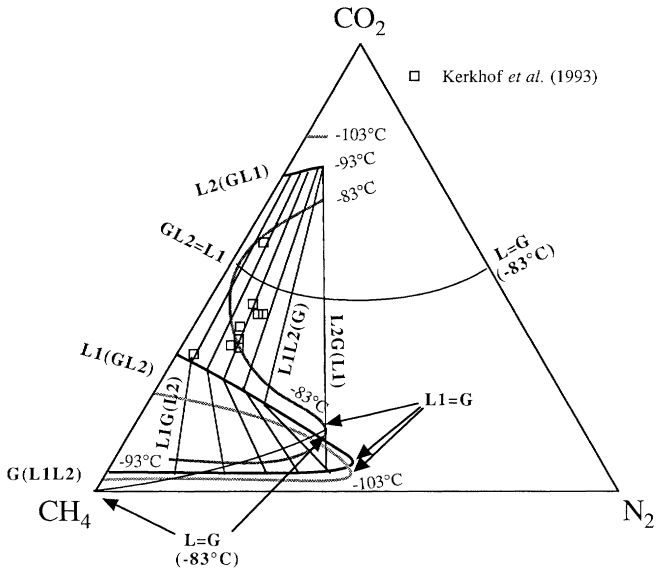

Fig. 11. Projection of the liquid-liquid-gas isotherms at -83.15°C, -93.15°C, -103.15°C and plotted measurement data from Van den Kerkhof *et al.* (1993) in the ternary CO_2-CH_4-N_2 polybaric diagram. Tie-lines for different compositions in the ternary system have been calculated by graphical determination of the intersection of L_1L_2 isotherms with L_1G isotherms calculated by the SRK EOS. Only the $L_1L_2(G)$ and $L_1G(L_2)$ tie-lines calculated at -93.15°C are shown here. Liquid-liquid-gas isotherms have been drawn by hand. $L_1(L_2G)$ isotherms meet the $G(L_1L_2)$ isotherms with increasing N_2 content. The calculated L = G critical curve at -83.15°C joins the L = G critical point of the CO_2-N_2 mixture to the $GL_1 = L_2$ critical point of the CO_2-CH_4-N_2 mixture.

the accuracy, but also the topology in some parts. Comparison with *vX* diagrams calculated by using the Heyen EOS (Darimont & Heyen, 1988; Heyen *et al.*, 1982) shows that our model significantly improves the accuracy of molar volume of the gas phase which was systematically underestimated by the Heyen EOS. This means that the internal pressure of a CO_2-CH_4 or CO_2-N_2 gas phase is overestimated using the *vX* diagrams of Heyen *et al.* (1982) and Darimont & Heyen (1988). Comparison with the diagram given by Herskowitz & Kisch (1984) as calculated with the Peng-Robinson EOS (Peng & Robinson, 1976) shows major differences in the $0.6 < XCH_4 < 0.7$ and 44 cm^3/mole $< v <$ 50 cm^3/mole regions. Contrary to our diagram, the L(S) isotherms in the *vX* diagram given by Herskowitz & Kisch (1984) are partly metastable and run above the L(SG) curve *e.g.* for the -70°C isotherm. This behaviour is not possible from a topological point of view and is not predicted by our model. According to our calculations, the L(S) isotherms must always end on the three-phase curve. Furthermore, L(S) isotherms for temperatures below -65°C are highly indicative for molar volume. The *vX* diagram of Herskowitz & Kisch (1984) also shows a higher molar volume maximum of the L(SG) than our diagram (64 instead of 58.5 cm^3/mole). This must have consequences for the interpretation of microthermometry data, notably for some of the "S2-type" : our diagram gives systematically higher molar volumes, for partial homogenization temperatures above -100°C and lower molar volumes ($v <$ 50 cm^3/mole) below -100°C. On the other hand, compositions obtained from microthermometry data are in good agreement for the CH_4-rich part in both diagrams and also with Raman analysis. By using the diagram of Herskowitz & Kisch (1984), Kisch & Van den Kerkhof (1991) found somewhat too high trapping pressures for the highest-density inclusions by isochore extrapolation. Our diagram would have given somewhat lower trapping pressures for these inclusions. The SL(G) tie-lines connecting solid and liquid at the three-phase equilibria partly run

above the L(SG) for the system CO_2-CH_4. These lines in part coincide for different temperatures and fluid inclusions points plotting on these tie-lines present both partial homogenization (SLG → SL) and "initial melting" by appearance of a gas bubble (SL → SLG). This phase behaviour is typical for CH_4-rich inclusions of "type H4" and has been frequently observed in fluid inclusions, notably in retrograde granulite rocks (Van den Kerkhof *et al.*, 1991, 1993). For binary CO_2-CH_4 mixtures, this type of phase behaviour is limited to compositions of 24-85 mole% CH_4 and molar volumes of 38-63 cm^3/mole, according to Herskowitz & Kisch (1984). The present model predicts much more limited ranges: 44-81 % CH_4 and 44-56 cm^3/mole. On the other hand, both observations and the model show that the H4 behaviour is strongly favoured with increasing N_2 contents.

Conclusion

vX properties of CO_2-CH_4 and CO_2-N_2 fluids for the complete ranges of composition and molar volumes have been calculated. The model shows good agreement with experimental data. The result has been obtained by using two thermodynamic models, namely the SRK and the LK EOS. In particular, better accuracies in the ranges of near-critical fluids have been obtained. Different projections of phase diagrams were constructed and appeared to predict well the complex phase behaviour as observed in fluid inclusions in the absence of water. We believe that, by using our model, molar volumes and compositions can be obtained with good accuracy from microthermometry and Raman data.

It is also possible to apply our model to ternary mixtures of the system CO_2-CH_4-N_2. Calculations on *vX* properties of this system will be done in the future. However, the results cannot be presented in simple phase diagrams. The conditions of the occurrence of the liquid-liquid-gas immiscibility at low temperatures have been discussed and calculated with our model; but it is felt that more basic experimental data are needed. The model presented here in this work will also be coupled with the model of mixed gas clathrates (Dubessy *et al.*, 1992) for the calculation of all phase transitions in the CO_2-CH_4-N_2-H_2O-NaCl system.

Acknowledgements : We have appreciated very much the careful reviews by Dr Grevel, Dr Vapnik and Kisch. We thank also C. Chopin and E.A.J. Burke for all their constructive comments. This work has been funded partially by Elf Aquitaine and CNRS.

References

Agrawal, G.M. & Laverman, R.J. (1974): Phase behavior of the methane-carbon dioxide system in the solid-vapor region. *Adv. Cryog. Eng.*, **19**, 327-338.

Al-Sahhaf, T.A., Kidnay, A.J., Sloan, E.D. (1983): Liquid-vapor equilibria in the N_2 + CO_2 + CH_4 system. *Ind. Eng. Chem. Fundam.*, **22**(4), 372-380.

Angus, S., Armstrong, B., De Reuck, K.M. (1976): Carbon dioxide. Vol. 3 of *International Thermodynamic Tables of the Fluid State*. Pergamon Press.

—, —, — (1978): Methane. Vol. 5 of *International Thermodynamic Tables of the Fluid State*. Pergamon Press.

—, —, — (1979): Nitrogen. Vol. 6 of *International Thermodynamic Tables of the Fluid State*. Pergamon Press.

Arai, Y., Kaminishi, G., Saito, S. (1971): The experimental determination of the P-V-T-X relations for the carbon dioxide-nitrogen and carbon dioxide-methane systems. *J. Chem. Eng. Jap.*, **4**(2), 113-122.

Asselineau, L., Bogdanic, G., Vidal, J. (1979): A versatile algorithm for calculating vapour-liquid equilibria. *Fluid Phase Equilibria*, **3**, 273-290.

Berdnikov, N.V. (1987): Thermobarogeochemistry: Precambrian metamorphic complexes of the Far East (Russia). Ph.D. Thesis, Institute of Tectonics and Geophysics, Khabarovsk, 115 p (in Russian).

Burruss, R.C. (1981): Analysis of fluid inclusions: phase equilibria at constant volume. *Amer. Jour. Sci.*, **281**, 1104-1126.

Chang, S.D. & Lu, B.C.Y. (1967): Vapor-liquid equilibria in the nitrogen-methane-ethane system. *Chem. Eng. Prog. Symp. Ser.*, **63**(81), 18-27.

Cines, M.R., Roach, J.T., Hogan, R.J., Roland, C.H. (1953): Nitrogen-methane vapor-liquid equilibria. *Chem. Eng. Prog. Symp. Ser.*, **49**(6), 1-100.

Darimont, A. & Heyen, G. (1988): Simulation des équilibres de phases dans le système CO_2-N_2. Applications aux inclusions fluides. *Bull. Minéral.*, **111**, 179-182.

Davalos, J., Anderson, W.R., Phelps, R.E., Kidnay, A.J. (1976): Liquid-vapor equilibria at 250 K for systems containing CH_4, C_2H_6 and CO_2. *J. Chem. Eng. Data*, **21**(1), 81-84.

Davis, J.A., Rodewald, N., Kurata, F. (1962): Solid-liquid-

vapor phase behavior of the methane-carbon dioxide system. *A.I.Ch.E. Journal*, **8**(4), 537-539.

Diamond, L. (1986): Hydrothermal geochemistry of late-metamorphic gold-quartz veins at Brusson, Val d'Ayas, Pennine Alps, NW. Italy. Unpubl. Ph.D. thesis, ETH-Zürich, 226 p.

Donnelly, H.G. & Katz, D.L. (1954): Phase equilibria in the carbon dioxide-methane system. *Ind. Eng. Chem.*, **46**(3), 511-517.

Dubessy, J., Thiéry, R., Canals, M. (1992): Modelling of phase equilibria involving mixed gas clathrates. Application to the determination of molar volume of the vapour phase and of the salinity of the aqueous solution in fluid inclusions. *Eur. J. Mineral.*, **4**, 873-884.

Herskowitz, M. & Kisch, H.J. (1984): An algorithm for finding composition, molar volume and isochores of CO_2-CH_4 fluid inclusions from Th and Tfm (for Th < Tfm). *Geochim. Cosmochim. Acta*, **48**, 1581-1587.

Heyen, G. (1981): A cubic equation of state with extended range of application. Second World Congress of Chemical Engineering. Ed. S.A. Newmann. Montreal: Ann Arbor Science, 1981. 175-185.

Heyen, G., Ramboz, C., Dubessy, J. (1982): Simulation des équilibres de phases dans le système CO_2-CH_4 en dessous de 50°C et de 100 bar. Application aux inclusions fluides. *C.R. Acad. Sci. Paris*, **294**, 203-206.

Huron, M.-J., Dufour, G.-N., Vidal, J. (1978): Vapour-liquid equilibrium and critical locus curve calculations with the Soave equation for hydrocarbons systems with carbon dioxide and hydrogen sulphide. *Fluid Phase Equilibria*, **1**, 247-265.

Hwang, S.-C., Lin, H.-M., Chappelear, P.S., Kobayashi, R. (1976): Dew point study in the vapor-liquid region of the methane + carbon dioxide system. *J. Chem. Eng. Data*, **21**(4), 493-497.

Kidnay, A.J., Miller, R.C., Sloan, E.D., Hiza, M.J. (1985): A review and evaluation of the phase equilibria, liquid-phase heats of mixing and excess volumes, and gas-phase PVT measurements for nitrogen + methane. *J. Phys. Chem. Ref. Data*, **14**(3), 681-694.

King, M.B. (1969): Phase equilibrium in mixtures. Pergamon Press, 585 p.

Kisch, H.J. & Van den Kerkhof, A.M. (1991): CH_4-rich inclusions from quartz veins in the Valley-and-Ridge province and the anthracite fields of the Pennsylvania Appalachians. *Am. Mineral.*, **76**, 230-240.

Kreglewski, A. & Hall, K.R. (1983): Phase equilibria calculated for the systems N_2 + CO_2, CH_4 + CO_2 and CH_4 + H_2S. *Fluid Phase Equilibria*, **15**, 11-32.

Krichevskii, I.R., Khazanova, N.E., Lesnevskaya, L.C., Sandalova, L. (1962): Liquid-gas equilibria in the nitrogen + carbon dioxide system at high pressures. *Khem. Prom.*, **3**, 169-171.

Lee, B.I. & Kesler, M.G. (1975): A generalized thermodynamic correlation based on three-parameter corresponding states. *A.I.Ch.E J.*, **21**, 510-527.

Mraw, S.C., Hwang, S.C., Kobayashi, R. (1978): Vapor-liquid equilibrium of the CO_2-CH_4 system at low temperatures. *J. Chem. Eng. Data*, **23**(2), 135-139.

Muirbrook, N.K. & Prausnitz, J.M. (1965): Multicomponent vapor-liquid equilibria at high pressures. Part I: experimental study of the nitrogen-oxygen-carbon dioxide system at 0°C. *A.I.Ch.E. J.*, **11**(6), 1092-1097.

Murphy, P.J. & Roberts, S. (1994): Laser Raman spectroscopy of differential partitioning in mixed-gas clathrates in H_2O-CO_2-N_2-CH_4 fluid inclusions: implications in microthermometry. *Geochim. Cosmochim. Acta*, in press.

Neumann, P.N.A. & Walch, W. (1968): Dampf / Flüssigkeits- Gleichgewicht CH_4-CO_2 im Bereich tiefer Temperaturen und kleiner CO_2 Molenbrüche. *Chem. Ing. Techn.*, **40**(5), 241-244.

Omar, H.O. (1962): Phase equilibria of some binary systems at low temperatures. Ph.D. Thesis. Univ. Leiden.

Parrish, W.R. & Hiza, M.J. (1974): Liquid-vapor equilibria in the nitrogen-methane system between 95 and 120 K. *Adv. Cryog. Eng.*, **19**, 300-308.

Peng, D.Y. & Robinson, D.B. (1976): A new two constants equation of state. *Ind. Eng. Chem. Fundam.*, **15**, 59-64.

Prausnitz, J.M. (1969): Molecular thermodynamics of fluid-phase equilibria. Prentice-Hall, Inc.

Schneider, G.M. (1978): High-pressure phase diagrams and critical properties of fluid mixtures. *Chem. Therm.*, **2**, 105-146.

Seitz, J.C., Pasteris, J.D., Wopenka, B. (1987): Characterization of CO_2-CH_4-H_2O fluid inclusions by microthermometry and laser Raman microprobe spectroscopy : inferences for clathrate equilibria. *Geochim. Cosmochim. Acta*, **51**, 1651-1664.

Soave, G. (1972): Equilibrium constants from a modified Redlich-Kwong equation of state. *Chem. Eng. Sci.*, **27**, 1197-1203.

Somait, F.A. & Kidnay, A.J. (1978): Liquid-vapor equilibria for systems containing N_2, CH_4 and CO_2. *J. Chem. Eng. Data*, **23**(4), 301-305.

Stryjek, R., Chapelear, P.S., Kobayashi, R. (1974): Low-temperature vapor-liquid equilibria of nitrogen-methane system. *J. Chem. Eng. Data*, **19**(4), 334-339.

Thiéry, R., Vidal, J., Dubessy, J. (1994): Phase equilibria modelling applied to fluid inclusions. Liquid-vapour equilibria and calculation of the molar

volume in the CO_2-CH_4-N_2 system. *Geochim. Cosmochim. Acta*, **58**, 1073-1082.

Van den Kerkhof, A.M. (1988): The system CO_2-CH_4-N_2 in fluid inclusions : theoretical modelling and geochemical applications. Ph.D. Thesis. Amsterdam (Free University), 206 p.

— (1990): Isochoric phase diagrams in the systems CO_2-CH_4 and CO_2-N_2: Application to fluid inclusions. *Geochim. Cosmochim. Acta*, **54**, 621-629.

Van den Kerkhof, A.M., Touret, J.L.R., Maijer, C., Jansen, J.B.H. (1991): Retrograde methane-dominated fluid inclusions from high-temperatures granulites of Rogaland, southwestern Norway. *Geochim. Cosmochim. Acta*, **55**(9), 2533-2543.

Van den Kerkhof, A.M., Frezzoti, M.-L., Talarico, F., Berdnikov, N.V. (1993): Metastable phase transitions in the system CO_2-CH_4-N_2 including immiscibility of the undercooled liquid (L_1L_2G): an example from granulites of the Wilson terrane, North Victoria Land (Antartica). European Current Research on Fluid Inclusions XII. *Archivum Mineralogiscze*. Warsaw: 1993. XLIX: 227-229.

Van Konynenburg, P.H. & Scott, R.L. (1980): Critical lines and phase equilibria in binary Van der Waals mixtures. *Phil. Trans. R. Soc.*, **A**, **298**, 495-540.

Vidal, J. (1978): Mixing rules and excess properties in cubic equations of state. *Chem. Eng. Sci.*, **33**, 787-791.

— (1983): Equations of state- Reworking the old forms. *Fluid Phase Equilibria*, **13**, 15-33.

— (1984): Phase equilibria and density calculations for mixtures in the critical range with simple equation of state. *Ber. Bunsenges. Phys. Chem.*, **88**, 784-791.

Zenner, G.H. & Dana, L.I. (1963): Liquid-vapor equilibrium compositions of carbon dioxide-oxygen-nitrogen mixtures. *Chem. Eng. Prog. Symp. Ser.*, **59**, 36-41.

Receveid 27 October 1993
Accepted 16 June 1994

Note added in proofs :
In Fig. 7b, read -63°C instead of -62°C for one of the LG(S) tie-line.